

## Chapter 8: Channel and Pipe Flow (Chap. 7 Bernard)

### Part 2: Pipe Flow

$R_e \sim 2000$  transition turbulence.

$$R_e = \frac{U_m D}{\nu} \quad U_m = \frac{Q}{A}$$

Fully developed flow:  $\underline{\bar{U}} = (\bar{U}(r), 0, 0) \rightarrow$  averaged streamwise momentum equation:

$$0 = -\frac{\partial \bar{p}}{\partial x} + \frac{1}{r} \frac{d}{dr} \left( \mu r \frac{d\bar{U}}{dr} - \rho r \overline{uv_r} \right) \quad (1)$$

Where  $r$  is the outward radial coordinate, i.e.,  $r = 0$  at the center of the pipe and  $r = R_0$  at the wall. Introduce wall coordinate:

$$y \equiv R_0 - r$$

Such that:

$$\bar{U}^*(y) = \bar{U}(R_0 - y)$$

However, the \* symbol will be dropped.

The wall shear stress:

$$\tau_w = \mu \frac{d\bar{U}}{dy}(0)$$

Which also defines  $R_\tau = \frac{U_\tau D}{\nu}$  where  $U_\tau = \sqrt{\frac{\tau_w}{\rho}}$  = friction velocity.

Integrating Eq. (1) over the pipe cross-section yields

$$0 = \int_0^{R_0} \int_0^{2\pi} -\frac{\partial \bar{p}}{\partial x} + \frac{1}{r} \frac{d}{dr} \left( \mu r \frac{d\bar{U}}{dr} - \rho r \overline{uv_r} \right) r dr d\theta$$

$$0 = -\pi R_0^2 \frac{\partial \bar{p}}{\partial x} - 2\pi R_0 \tau_w$$

$$-\pi R_0^2 \frac{\partial \bar{p}}{\partial x} = 2\pi R_0 \tau_w \quad (2)$$

Since

$$\frac{d\bar{U}}{dr}(R_0) = -\frac{d\bar{U}}{dy}(0)$$

And

$$\overline{v_r}(0) = \overline{uv_r}(0) = \overline{uv_r}(R_0) = 0$$

Eq. (2) shows that  $\frac{\partial \bar{p}}{\partial x} = f(\tau_w)$ .

The volumetric flow rate:

$$Q = 2\pi \int_0^{R_0} \bar{U}(r) dr$$

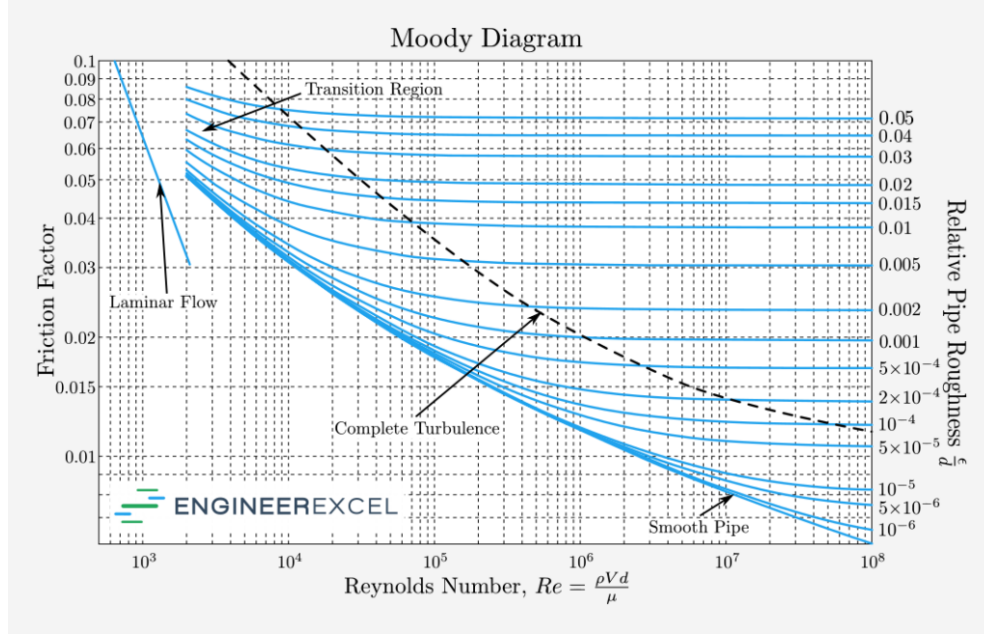
can be determined once  $\bar{U}(r)$  is known, which determines the averaged velocity  $U_m = Q/A$  where  $A = \pi R_0^2$  and defines the Reynolds number

$$Re = \frac{U_m D}{\nu}$$

Define friction factor for pipe flow  $f$  as:

$$f = \frac{\Delta \bar{p}}{\Delta x} \frac{2D}{\rho U_m^2} = 8 \frac{R_\tau^2}{R_e^2} = \frac{8\tau_w}{\rho U_m^2} \quad (3)$$

The Moody diagram can be used to find values of  $f(Re)$ .



Current analysis presumes that the pipe is smooth. For engineering applications, it is necessary to consider  $f(Re, \frac{\epsilon}{d})$ , where  $\frac{\epsilon}{d}$  represents the relative pipe roughness (see Appendix).

Alternatively explicit formulas are available for smooth and rough pipes, e.g.:

For  $Re < 10^5$ , the Blasius smooth pipe friction law

$$f = 0.266 R_e^{-1/4}$$

And substituting this into Eq. (3) gives a relationship between  $R_\tau$  and  $R_e$

$$R_\tau = 0.182 R_e^{7/8}$$

Previous channel flow analysis neglected outer layer, which should be included for pipe and especially BL flows.

In viscous sublayer ( $y^+ < 5$ ):

$$\overline{U}^+ = y^+$$

And log law valid for intermediate layer of pipe flow.

For high Re pipe flow, central core mean velocity cannot be scaled using viscosity, so similarity is achieved using the velocity defect law:

$$\frac{\overline{U}_{cl} - \overline{U}(y)}{U_\tau} = g(\xi)$$

Where  $\overline{U}_{cl}$  = mean centerline velocity and  $\xi \equiv y/R_0$  is a similarity variable. In practice, this equation is found to work also in most of the intermediate region.

If velocity defect law applies in overlap region, then:

$$f(y^+) = \overline{U}^+ = \frac{\overline{U}_{cl}}{U_\tau} - g(\xi) \quad (4)$$

Differentiating Eq. (4) with respect to  $y$  gives

$$\frac{df}{dy^+}(y^+) \frac{U_\tau}{\nu} = -\frac{dg}{d\xi}(\xi) \frac{1}{R_0}$$

$$y^+ = \frac{U_\tau y}{\nu}$$

And multiplying both sides of the equation by  $y$  gives:

$$y^+ \frac{df}{dy^+}(y^+) = -\xi \frac{dg}{d\xi}(\xi) \quad (5)$$

LHS only  $f(y^+)$  and RHS only  $f(\xi)$ ; thus both sides must equal and constant. Setting the constant to be  $1/k$ :

$$y^+ \frac{df}{dy^+}(y^+) = \frac{1}{k}$$

Integration gives the log law:

$$\bar{U}^+ = k^{-1} \log y^+ + B$$

i.e., using velocity defect law in intermediate layer recovers log-law.

New high Re data shows  $k = 0.42$ ,  $B = 5.6$  for  $600 \leq y^+ \leq 0.12R_0^+$  vs. historical 4.1 and 5.2.

The details of the velocity defect law for outer flow will be analyzed for BL flow.

In the region beyond the viscous layer, up to  $y^+ \sim 300$ , a power law gives:

$$\overline{U}^+ = 8.48(y^+)^{0.142}$$

For  $5 < y^+ < 300$ .

This should be compared with previously defined composite sub-layer, blending layer, and logarithmic-overlap formulas:

$$U^+ = y^+ - e^{-\kappa B} \left[ e^{\kappa U^+} - 1 - \kappa U^+ - \frac{(\kappa U^+)^2}{2} - \frac{(\kappa U^+)^3}{6} \right]$$

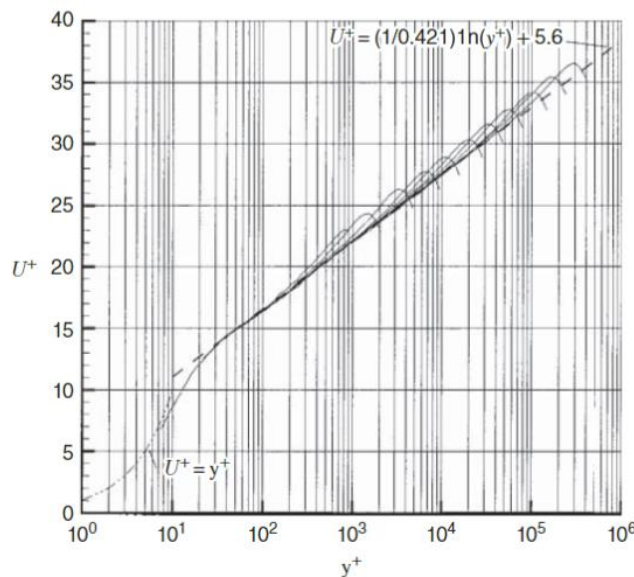


Figure 7.18 Mean velocity profiles in pipe flow [6] showing the collective approach to a log law. The curves are for Reynolds numbers between  $R_e = 31 \times 10^3$  and  $R_e = 18 \times 10^6$ . Reprinted with permission of Cambridge University Press.

## Power Law

Early studies showed that power laws can represent flow behavior over the entire pipe cross-section:

$$\frac{\bar{U}}{U_{cl}} = \left( \frac{y}{R_0} \right)^{1/n}$$

Where  $n$  increases with  $Re$ , shows good fit with data, but cannot provide  $\tau_w$ .

Taking a derivative of the power law gives:

$$\frac{d\bar{U}}{dy} = \frac{U_{cl}}{n} \left( \frac{y}{R_0} \right)^{\frac{1}{n}-1}$$

Where experimental fits show that  $n \sim 6 - 10$ , such that  $\frac{1}{n} - 1 \sim - (0.85 - 0.9)$ .

Therefore, e.g., for  $n = 10$ :

$$\frac{d\bar{U}}{dy}(0) \sim \frac{U_{cl}}{n} \left( \frac{R_0}{y} \right)^{0.9}$$

Showing that the shear stress approaches  $\infty$  as  $y \rightarrow 0$ .

Linear-log plots of power law show good fit to the data for range of  $n$ :

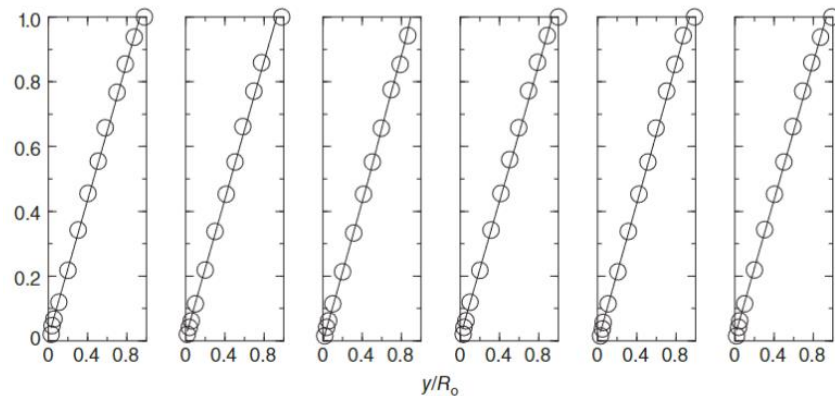


Figure 7.19 Plots of  $(\bar{U}/\bar{U}_{max})^{1/n}$  in pipe flow for empirically fitted exponents,  $n$ . From left to right  $n = 6.0, 6.6, 7.0, 8.8, 10.0$ , and the Reynolds numbers are  $4 \times 10^3, 2.3 \times 10^4, 1.1 \times 10^5, 1.1 \times 10^6, 2 \times 10^6$ , and  $3.2 \times 10^6$ . From [25], p. 563.

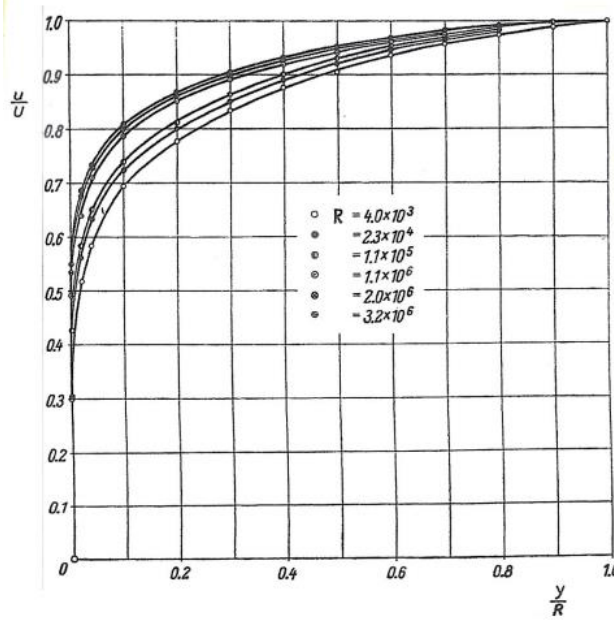


Fig. 20.2. Velocity distribution in smooth pipes for varying Reynolds number, after Nikuradse [45]

Subsequently, power laws were generalized to include not only inner law variables ( $y, \tau_w, \nu, \rho$ ) but also outer law variable  $R_0$ , i.e.,  $d\bar{U}/dy = f(y, \tau_w, \nu, \rho, R_0)$  for the intermediate layer to include dependence on  $\nu$  and  $R_0$ , i.e., generalization of the log law approach, but in this case not independent of  $Re$  (partial similarity).

Dimensional analysis gives:

$$\frac{d\bar{U}}{dy} = \frac{U_\tau}{y} f(y^+, R_\tau) \quad (6)$$

But since  $R_\tau$  is related to  $R_e$ , Eq. (6) can be rewritten as:

$$\frac{d\bar{U}}{dy} = \frac{U_\tau}{y} f(y^+, R_e) \quad (7)$$

If  $f = \text{constant}$ , log law is implied, alternatively if  $f$  obeys a power law:

$$f(y^+, R_e) = \beta^*(R_e)(y^+)^{\alpha(R_e)} \quad (8)$$

For large  $y^+$  and  $R_e$ .



Both  $\bar{U}^+$  and  $f$  will follow power laws after integration of Eq. (7) using (8).

$$d\bar{U} = \frac{U_\tau}{y} \beta^*(R_e)(y^+)^{\alpha(R_e)} dy$$

$$d\bar{U}^+ = \beta^*(y^+)^{\alpha-1} dy^+$$

$$\int_{\bar{U}^+(0)}^{\bar{U}^+(y^+)} d\bar{U}^+ = \beta^* \int_0^{y^+} (y^+)^{\alpha-1} dy^+$$

$y^+ = \frac{U_\tau y}{\nu}$ $dy^+ = \frac{U_\tau}{\nu} dy$ $\bar{U}^+ = \frac{\bar{U}}{U_\tau}$
--

Applying BC at the wall gives:

$$\bar{U}^+(y^+) = \frac{\beta^*}{\alpha} (y^+)^{\alpha}$$

$$\bar{U}^+(y^+) = \beta(R_e)(y^+)^{\alpha(R_e)} \quad (9)$$

Where  $\beta$  is defined from  $\alpha$  and  $\beta^*$  after the integration, i.e.,  $\beta = \beta^* / \alpha$ .

To determine a form of  $\alpha(R_e)$ , consider behavior of Eq. (9) as  $\nu \rightarrow 0$ . If  $\frac{\partial \bar{p}}{\partial x}$  is constant,  $\tau_w$  remains constant as  $\nu \rightarrow 0$ , and so does  $U_\tau$ .

Since  $\bar{U}$  is bounded,  $\bar{U}^+$  is bounded, so LHS of Eq. (9) is bounded as  $\nu \rightarrow 0$ .

Consequently, RHS must be bounded as  $y^+ \rightarrow \infty$  and  $R_e \rightarrow \infty$ .

Noting the identity

$$(y^+)^{\alpha(R_e)} = e^{\alpha(R_e) \log y^+}$$

Using this reasoning  $\alpha(R_e)$  is assumed of the form:

$$\alpha(R_e) = \frac{\alpha_1}{\log R_e}$$

where  $\alpha_1 = \text{constant}$  reaches a non-zero limit for high  $Re$ :

$$\alpha(R_e) \log y^+ = \alpha_1 \log \left( \frac{y^+}{Re} \right) \rightarrow -\alpha_1 \text{ for } Re \rightarrow \infty$$

and gives good agreement with experiments. It is assumed that  $\beta(R_e)$  shows the same dependence on  $R_e$  as  $\alpha$ :

$$\beta(R_e) = \beta_0 + \frac{\beta_1}{\log R_e}$$

Where  $\beta_0$  and  $\beta_1$  are constants.

It is then derived that:

$$\overline{U}^+(y^+) = \left( \beta_0 + \frac{\beta_1}{\log R_e} \right) (y^+)^{\frac{\alpha_1}{\log R_e}} \quad (10)$$

Where the appearance of  $R_e$  in the form of its logarithm means that if  $R_e$  is replaced by  $\gamma R_e \rightarrow \log \gamma R_e = \log \gamma + \log R_e$ , which converges to  $\log R_e$  as  $R_e \rightarrow \infty$ .

$\alpha_1$  and  $\beta_1$  should have universal form and together with  $\beta_0$  are determined by empirical fit, comparing with EFD data.

For  $4 \times 10^3 \leq R_e \leq 3.24 \times 10^6$ :  $\alpha_1 = 1.5$ ,  $\beta_0 = 0.578$ , and  $\beta_1 = 2.5$ .

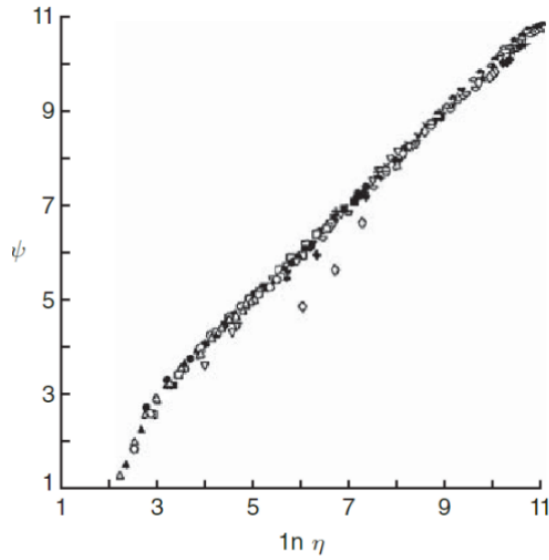


**Figure 7.20**  $\psi$  vs.  $\log y^+$  where  $\eta \equiv y^+$  in this figure. Data are taken from 16 different Reynolds numbers from  $4 \times 10^3$  to  $3.24 \times 10^6$  measured in [29]. From [31]. Reprinted with permission from ASME International.

$$\psi \equiv \frac{\log R_e}{\alpha_1} \log \left( \frac{\overline{U}^+}{\beta_0 + \frac{\beta_1}{\log R_e}} \right)$$

From Eq. (10):

$$\frac{\overline{U}^+}{\beta(R_e)} = (y^+)^{\frac{\alpha_1}{\log R_e}} = a$$

$$\log a = \frac{\alpha_1}{\log R_e} \log y^+ \rightarrow \log y^+ = \frac{\log R_e}{\alpha_1} \log a = \psi$$

i.e., Eq. (10) is equivalent to  $\psi = \log y^+$ .

Since the power law is meant to cover larger region of the pipe than the log law, it can be used to explain large  $y^+$  departure from log law.

Streamwise normal RS  $\overline{u^2}$  for high Re data shows 2<sup>nd</sup> peak in addition to peak at  $y^+ = 15$ , but reason for this is still under discussion.

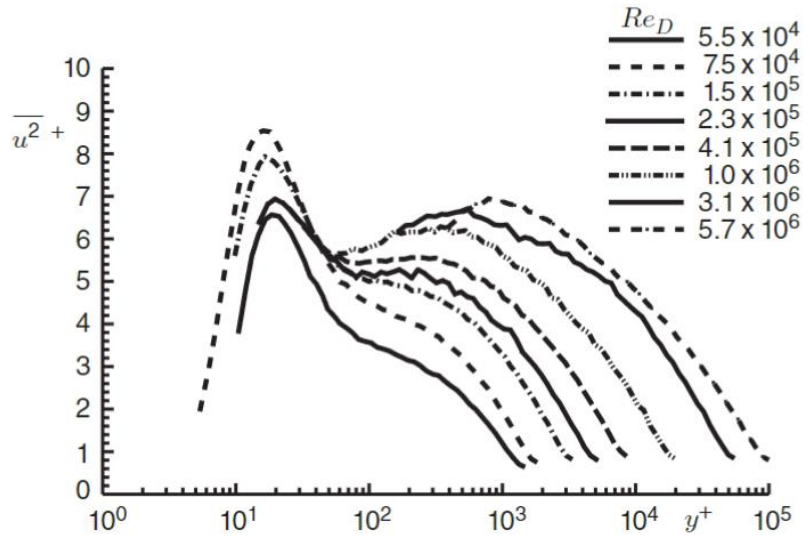


**Figure 7.21** Streamwise velocity variance at high Reynolds numbers in pipe flow [32]. Reprinted with permission of Cambridge University Press.

## Appendix

Roughness

$$k = \text{roughness height}$$

$$k^+ = \frac{k u^*}{\nu}$$

$k^+ < 4$  hydraulically smooth

$4 < k^+ < 60$  transitional roughness  $f(Re)$

$k^+ > 60$  fully rough  $\neq f(Re)$

$$\sigma/\kappa^+ = \frac{1}{\kappa} \ln y^+ + B + \frac{2\pi}{\kappa} W(y/\delta) - \Delta U^+$$

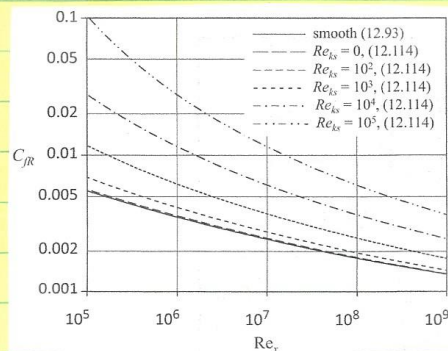
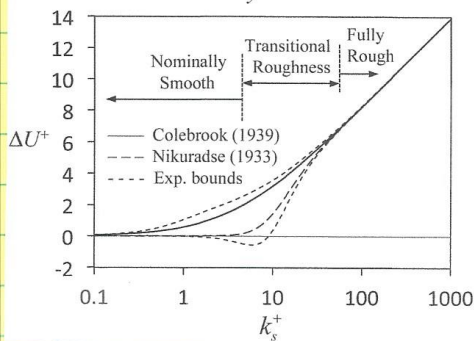
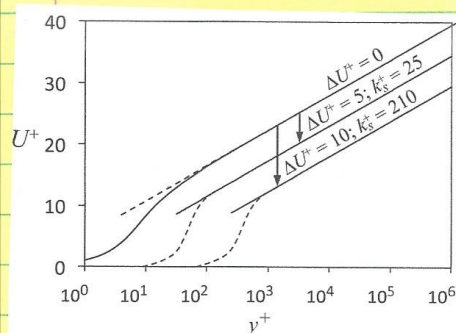
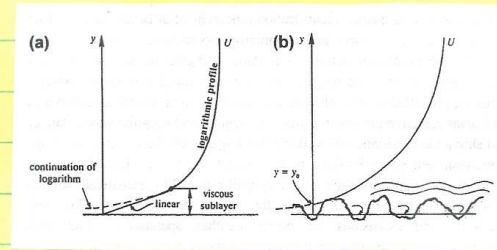


**FIGURE 12.25** Rough surface skin friction coefficient,  $C_{fR}$ , for a zero-pressure-gradient flat-plate turbulent boundary layer vs.  $Re_x$ , the Reynolds number based on downstream distance. The solid curve corresponds to (12.93) evaluated using log-law constants  $\kappa=0.39$  and  $B=4.3$  (as recommended by Marusic et al., 2013). The dashed and dash-dot curves come from implicit evaluation of (12.114) for equivalent-sand-grain roughness-height Reynolds numbers of  $Re_{ks} = 0, 10^2, 10^3, 10^4$ , and  $10^5$ . The  $C_{fR}$  values produced by (12.114) agree within engineering accuracy ( $\pm 5\%$  or so) with prior rough-plate results.